An intercomparison of radiation partitioning models in vineyard canopies

C. K. Parry[1] · H. Nieto[2] · P. Guillevic[3] · N. Agam[4] · W. P. Kustas[5] · J. Alfieri[5] · L. McKee[5] · A. J. McElrone[1,6]

Abstract

Multiple radiation transfer models with unique clumping indices (a total of five approaches) were evaluated on two Pinot Noir vineyards in Central California over 3 years. In the first approach, a basic clumping index meant for heterogeneous randomly placed clumped canopies was combined with the Campbell and Norman transfer model (C&N–H). The other four approaches, namely, the Campbell and Norman with rectangular hedgerow clumping index (C&N–R), Campbell and Norman with a geometric elliptical hedgerow model (C&N–E), the 4-stream scattering by arbitrary inclined leaves model (4SAIL) with row-crop clumping index, and the discrete anisotropic radiative transfer (DART) models, account for the unique canopy coverage distribution of the vineyard row-structured canopies. Each modeling approach varied in its complexity to predict transmitted solar radiation at ground level and the outputs were compared to solar radiation observed at the surface with an array of pyranometers. All five modeling approaches showed good agreement with the observed values [correlation coefficients (r) ranged from 0.95 to 0.97]. Model performance varied throughout the season due to their sensitivity to canopy growth. Although r values showed good agreement among all approaches, the C&N–E and DART models showed a better "goodness of fit" with lower root mean squared and bias values.

✉ A. J. McElrone
Andrew.McElrone@ars.usda.gov

1   USDA-ARS Crops Pathology and Genetics Research Unit, Davis, CA 95616, USA

2   Efficient Use of Water in Agriculture Program, Institut de Recerca i Tecnologia Agroalimentàries (IRTA), Lleida, Spain

3   Department of Geographical Sciences, University of Maryland, Terrestrial Information Systems Laboratory, NASA Goddard Space Flight Center, Greenbelt, MD 20771, USA

4   Blaustein Institutes for Desert Research, Ben-Gurion University of the Negev, Sede-Boqer Campus, 84990 Beersheba, Israel

5   USDA ARS, Hydrology and Remote Sensing Laboratory, Beltsville, MD 20705-2350, USA

6   Department of Viticulture and Enology, University of California, Davis, CA 95616, USA

Introduction

Accurate radiation transfer models are important for energy balance models that estimate crop evapotranspiration (ET) and for crop production models, which depend on accurate canopy radiation interception estimates for modeling canopy photosynthesis (Nouvellon et al. 2000; Chen et al. 2003). Radiation at the surface can be either predicted with models or observed directly, but direct measurement of transmitted radiation through a canopy is not practical for implementation over large areas of interest. The Campbell and Norman (1998) radiation transfer model has been widely used to estimate shortwave transmittance and reflectance of vegetated surfaces for use in energy balance models to estimate ET (Kustas and Norman 1999; Anderson et al. 2005; Li et al. 2005; French et al. 2007), canopy stomatal conductance, and canopy water stress (Blonquist et al. 2009).

For a hedge row crop with partial canopy cover, the model needs to account for radiation that will be directly transmitted to the surface through the inter row space as well as the radiation transmitted through canopy gaps and through the canopy leaves. The non-random spatial distribution of row-crop vegetation has been commonly accounted for using either a semi-empirical clumping

index approach (e.g., Kustas and Norman 1999; Anderson et al. 2005) or by modeling the canopy using simple geometric shapes such as hedgerows (e.g., Annandale et al. 2004; Pieri 2010a, b). Colaizzi et al. (2012) used a geometric elliptical approach coupled with the Campbell and Norman (1998) radiation transfer model to account for the spatial distribution of row crops similar to Charles-Edwards and Thornley (1973) and Annandale et al. (2004). Colaizzi et al. (2012) evaluated the Campbell and Norman (1998) procedure to calculate individual radiation balance components for corn, sorghum and cotton. Similar efforts have not been applied to the unique geometry of grapevine canopies and vineyards. Here, we used the Campbell and Norman (C&N) radiation transfer model with three unique clumping indices to predict transmitted solar radiation for a vineyard surface. The clumping indices included: (1) a basic clumping index for heterogeneous clumped canopies (C&N–H); (2) a rectangular hedgerow clumping index (C&N–R); and (3) a geometric elliptical hedgerow index (C&N–E). We also evaluated two other radiation transfer models, the 4-stream scattering by arbitrary inclined leaves (4SAIL) model (Verhoef et al. 2007) and the discrete anisotropic radiative transfer (DART) model (Gastellu-Etchegorry et al. 1996, 2015; Guillevic and Gastellu-Etchegorry 1999; Gastellu-Etchegorry 2008, 2017). 4SAIL simulates the absorption, scattering and transmission processes of a homogeneous turbid plant canopy in both the optical and thermal infrared regions. The DART model simulates radiative transfer from the visible to the thermal infrared portions of the electromagnetic spectrum within heterogeneous canopies characterized by a three-dimensional (3-D) structure. The radiation propagation is tracked with a ray-tracing approach combined with the discrete ordinate method, i.e., radiation can only propagate along a prescribed number of discrete directions. The model has been used to predict surface directional radiance of natural and urban surfaces and the 3-D distribution of radiative energy within the canopy over narrow or wide spectral domains.

The objective of the current study was to evaluate these five radiation transfer modeling approaches applied to two Pinot Noir vineyards to determine which model most accurately predicts shortwave radiation transferred below a vineyard canopy surface. Results were compared to solar radiation observed at the surface in each vineyard site. Model evaluation was performed by assessing model agreement between predicted and observed shortwave radiation transferred through the canopy and to the surface using statistical metrics. Model evaluation also consisted of a sensitivity analysis of each model to key input parameters that were individually increased or decreased by 10 or 30% for clear sky and cloudy conditions.

Materials and methods

Field measurements

As part of the USDA-ARS Grape Remote-Sensing Atmospheric Profile and Evapotranspiration eXperiment (GRAPEX), two Pinot Noir vineyards, located at the border of Sacramento and San Joaquin counties in California, were instrumented in 2013, 2014, and 2015 with eddy-covariance flux towers and in-field ground measurements of soil moisture and temperature. Additional ground, airborne, and satellite remote-sensing data were collected along with ground biophysical data during intensive observation periods (IOPs). These IOPs covered two-to-four phenological stages (i.e., around bloom, canopy fill, veraison, and harvest) each year. The larger, northern field (site 1; 34.4 ha) contains more mature grapevines (7–8 years in 2014), while the vines in the smaller southern field (site 2; 21 ha) were 4–5 years in 2014. The height of the vines ranged between 2 and 2.5 m, row spacing was ~ 3.35 m, and average vine spacing along the row was 1.52 m. Due to the trellis design and vine management, the majority of vegetative growth was located within the upper 1/2–1/3 of the vine by the end of the season. Vines were drip irrigated using an irrigation schedule based on recommendations from E&J Gallo Irrigation management. Pruning activities, cover crop mowing, and application of agrochemicals were managed according to standard industry practices. Both fields have east–west row orientation. Because winds are typically from the west in this area, the towers were located on the eastern edge of the fields, such that the dominant fetch for both towers typically lies within the target field boundaries.

In both sites, we measured transmitted solar radiation in the canopy inter-row using a transect of five-to-eight upward facing hemispherical view radiometers [Kipp and Zonen models CMP3 (285–3000 nm) and CMP11 (270–3000 nm), Eppley Laboratory Inc. Newport RI, Model PSP (295–2800 nm) and Apogee Instruments Inc. Logan, Utah model SP 212 (360–1120 nm)] that were evenly spaced across the row middle. These were part of the ground measurements taken during the IOPs. Measurements were taken every 10 s and averaged to 15 min. Details of the radiation measurements are provided in Kustas et al. (2018) (Supplemental Fig. 1). Canopy height (h_c), width (w_c), and field leaf area index (LAI) were measured at various locations in each of the two vineyard sites during each IOP, and included destructive sampling and indirect estimates based on light extinction.

Overview of the radiation transfer models

Transmitted solar radiation to the surface was estimated for grapevines using multiple radiation transfer models with unique clumping indices providing a total of five approaches,

and these results were compared to solar radiation observed at the surface in each vineyard site. For the first approach, a basic clumping index meant for heterogeneous clumped canopies was combined with the Campbell and Norman transfer model (C&N–H). The other four approaches Campbell and Norman with rectangular hedgerow clumping index (C&N–R), Campbell and Norman with a geometric elliptical hedgerow model (C&N–E), 4SAIL with rectangular hedgerow clumping index (4SAIL-R), and the discrete anisotropic radiative transfer (DART) model account for the unique vine canopy density distribution (both vertical and horizontal) as well as orientation. Details for each approach and associated clumping indices are described below.

Campbell and Norman radiation transfer model

Transmitted shortwave irradiance (TR_S) beneath the crop canopy was calculated as

$$TR_S = R_{SO}\tau_C, \tag{1}$$

where R_{SO} is global shortwave irradiance (W m^{-2}) and τ_C is transmittance of shortwave radiation through the canopy.

Calculating the transmittance of shortwave radiation through the canopy also depends on the wavelength due to vegetation absorbing a greater portion of the photosynthetically active radiation (PAR, 400–700 nm spectrum) than near-infrared radiation (NIR, 700–2500 nm spectrum) wavelengths. The transmittance τ_C is partitioned into four components each having a view factor for either direct beam or diffuse irradiance and a weighing factor for PAR or NIR.

The transmittance of shortwave radiation through the canopy for a horizontally homogeneous canopy is defined as

$$\tau_C = F_{PAR}[W_{DIR,PAR}\tau_{C,DIR,PAR} + W_{DIFF,PAR}\tau_{C,DIFF,PAR}]$$
$$+ F_{NIR}[W_{DIR,NIR}\tau_{C,DIR,NIR} + W_{DIFF,NIR}\tau_{C,DIFF,NIR}], \tag{2}$$

where F_{PAR} and F_{NIR} are the fractions of shortwave radiation in the PAR and NIR bands, respectively, which are dependent on sun direction, $W_{DIR,PAR}$ and $W_{DIFF,PAR}$ are the weighing factors for direct (DIR) and diffuse (DIFF) radiation, respectively, in the PAR wavelengths, $W_{DIR,NIR}$ and $W_{DIFF,NIR}$ are the weighing factors for DIR and DIFF, respectively, in the NIR wavelengths, $\tau_{C,DIR,PAR}$ and $\tau_{C,DIFF,PAR}$ are the transmittance for DIR and DIFF, respectively, in the PAR wavelengths, and $\tau_{C,DIR,NIR}$ and $\tau_{C,DIFF,NIR}$ are the transmittance for DIR and DIFF, respectively, in the NIR wavelengths.

F_{PAR} in this study was set constant at 0.457 consistent with the values used in Colaizzi et al. (2012) in Bushland, Texas, and other locations in the western United States (McCree 1972; Meek et al. 1984). F_{NIR} is calculated as the compliment unit of F_{PAR} (i.e., $F_{NIR} = 1.0 - F_{PAR}$).

The weighing factors $W_{DIR,PAR}$ and $W_{DIR,NIR}$ were calculated following the procedure outlined in Colaizzi et al. (2012) which followed the procedure of Weiss and Norman (1985):

$$W_{DIR,PAR} = \left(\frac{R_{SO,DIR}}{R_{SO}}\right) a \left(\frac{R_S}{R_{SO}}\right)^b \tag{3}$$

$$W_{DIR,NIR} = \left(\frac{R_{SO,DIR}}{R_{SO}}\right) c \left(\frac{R_S}{R_{SO}}\right)^d, \tag{4}$$

where $R_{SO,DIR}$ and R_{SO} (W m^{-2}) are the direct-beam and global solar irradiance for clear skies, respectively (calculated according to Allen 2005) and R_S is the measured incoming solar irradiance (W m^{-2}). $W_{DIFF,PAR}$ and $W_{DIFF,NIR}$ are the unit complement of $W_{DIR,PAR}$ and $W_{DIR,NIR}$, respectively. Slight modifications to the procedure were done using the empirical constants of Weiss and Norman (1985) ($a = 0.90$, $b = 0.70$, $c = 0.88$, $d = 0.68$), instead of the derived constants determined at the Colaizzi et al. (2012) study location of Bushland, Texas.

The direct-beam PAR transmittance ($\tau_{C,DIR,PAR}$) was calculated following the equations of Campbell and Norman (1998) for a single layer crop:

$$\tau_{C,DIR,PAR} = \frac{(\rho_{C,PAR}^{*2} - 1)\exp(-\sqrt{\zeta_{PAR}}K_{BE}LAI)}{[(\rho_{C,PAR}^{*}\rho_{S,PAR} - 1) + \rho_{C,PAR}^{*}(\rho_{C,PAR}^{*} - \rho_{S,PAR})\exp(-2\sqrt{\zeta_{PAR}}K_{BE}LAI)]}, \tag{5}$$

where $\rho_{C,PAR}^{*}$ is the beam PAR reflection coefficient for a deep canopy with non-horizontal leaves, ζ_{PAR} is the PAR absorption of the leaves, K_{BE} is the extinction coefficient for direct-beam radiation (per LAI unit), LAI is the leaf area index (m^2 m^{-2}), and $\rho_{S,PAR}$ is the soil reflectance in the PAR. The increased downwelling radiation that is reflected by the soil and then scattered by the canopy back down to the ground surface is accounted for in the $\rho_{C,PAR}^{*}$ and $\rho_{S,PAR}$ terms. Campbell and Norman (1998) reported the Goudriaan (1988) equation for $\rho_{C,PAR}^{*}$:

$$\rho_{C,PAR}^{*} = \frac{2K_{BE}\rho_{HOR,PAR}}{K_{BE} + 1}, \tag{6}$$

where $\rho_{HOR,PAR}$ is the beam reflection coefficient for a canopy with horizontal leaves calculated as

$$\rho_{\text{HOR,PAR}} = \frac{1 - \sqrt{\zeta_{\text{PAR}}}}{1 + \sqrt{\zeta_{\text{PAR}}}}. \tag{7}$$

Direct-beam NIR transmittance ($\tau_{\text{C,DIR,NIR}}$) as used in Eq. (2) above was calculated identically to $\tau_{\text{C,DIR,PAR}}$ except ζ_{PAR} was replaced with ζ_{NIR} in Eqs. (5) and (6). This results in $\rho_{\text{C,NIR}}{}^*$ and $\rho_{\text{HOR,NIR}}$ terms. In addition, $\rho_{\text{S,PAR}}$ was replaced with $\rho_{\text{S,NIR}}$ in Eq. (5). Diffuse transmittance ($\tau_{\text{C,DIFF,PAR}}$ and $\tau_{\text{C,DIFF,NIR}}$) was calculated by numerically integrating $\tau_{\text{C,DIR,PAR}}$ and $\tau_{\text{C,DIR,NIR}}$, respectively, over a half-sphere. The canopy beam extinction (K_{BE}) was calculated based on the ellipsoidal LADF of Campbell (1990):

$$K_{\text{BE}} = \frac{\sqrt{X_{\text{E}}^2 + \tan^2\theta_{\text{S}}}}{X_E + 1.774(X_E + 1.182)^{-0.733}}, \tag{8}$$

where X_{E} is the ratio of horizontal to vertical projected unit of area of leaves, and θ_{S} is the solar zenith angle. The X_{E} parameter quantifies the average leaf angle and is specific to species and its leaf angle distribution. For this study, a spherical leaf angle distribution ($X_{\text{E}} = 1.0$) was assumed.

Soil reflectance ($\rho_{\text{S,PAR}}$ and $\rho_{\text{S,NIR}}$) was assumed to be 0.14 and 0.25 for this study, similar to values suggested by Campbell and Norman (1998) and reported in the literature (Colaizzi et al. 2012; Howell et al. 1993; Tunick et al. 1994).

It is important to note that although transmittance is not directly dependent on the solar zenith angle (θ_{S}), it is indirectly dependent on θ_{S} through the terms K_{BE} (Eq. 8) and $\rho_{\text{C,PAR}}$ (Eq. 4).

Clumping indices combined with Campbell and Norman model

Clumping index for randomly placed isolated canopies (C&N–H)

Similar to Colaizzi et al. (2012) model, $\tau_{\text{C,DIR,PAR}}$ uses effective values of $\text{LAI}_{\text{eff}} = \Omega F$ depending on solar incidence angle:

$$\tau_{\text{C,DIR,PAR}} = \frac{(\rho_{\text{C,PAR}}{}^{*2} - 1)\exp(-\sqrt{\zeta_{\text{PAR}}} K_{\text{BE}}\Omega F)}{[(\rho_{\text{C,PAR}}{}^* \rho_{\text{S,PAR}} - 1) + \rho_{\text{C,PAR}}{}^*(\rho_{\text{C,PAR}}{}^* - \rho_{\text{S,PAR}})\exp(-2\sqrt{\zeta_{\text{PAR}}} K_{\text{BE}}\Omega F)]} \tag{9}$$

and $\tau_{\text{C,DIR,PAR}}$ calculated using Eqs. (1)–(5).

In this case, we use the clumping index as defined in Kustas and Norman (1999). First, the nadir viewing clumping index $\Omega(0)$ is calculated as

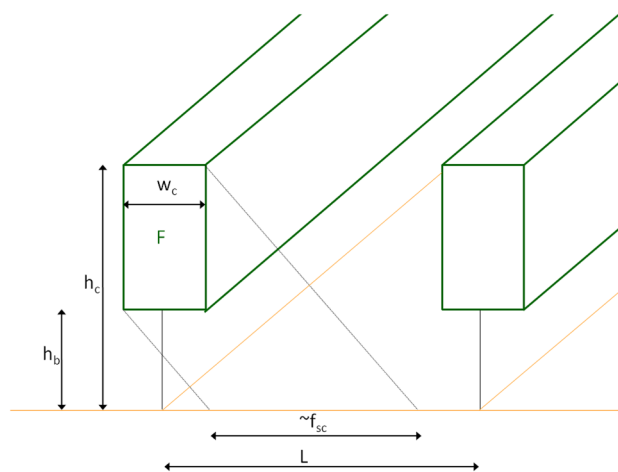$$\Omega(0) = \frac{\ln((1 - f_{\text{c}}) + (f_{\text{c}} * f_{\text{gap}}))}{-K_{\text{BE}}(0) * \text{LAI}}, \tag{10}$$

Fig. 1 Canopy model for estimating the clumping index in row crops, F is the leaf area index, L is the distance between rows, h_{c} is the canopy height, h_{b} is the height of the canopy above ground, and w_{c} is the canopy width

where $f_{\text{c}} = w_{\text{c}}/L$, where L is the row separation (m) f_{gap} is the area, where soil is seen through the gaps of the canopy viewing at nadir:

$$f_{\text{gap}} = \exp(-K_{\text{BE}}(0) * \text{LAI}). \tag{11}$$

Then, the off-nadir clumping index $\Omega(\theta)$ is calculated using the empirical formula for randomly placed canopies proposed by Campbell and Norman (1998) and Kustas and Norman (1999):

$$\begin{aligned} \Omega(\theta) &= \frac{\Omega(0)}{\Omega(0) + [1 - \Omega(0)]\exp[-2.2(\theta)^p]} \\ p &= 3.80 - 0.46D \quad 1 \leqslant D \leqslant 3.34 \\ D &= \frac{h_{\text{c}} - h_{\text{b}}}{w_{\text{c}}}, \end{aligned} \tag{12}$$

where h_{c} is the canopy height and w_{c} is the canopy width that is placed above the ground at h_{b} (i.e., the height of the first living branch) (see labelling scheme in Fig. 1).

Clumping index for rectangular hedgerow (C&N–R)

We developed a simplified method to derive the clumping index in row crops such as vineyards. The new clumping index is based on the ideas of the geometric model by Colaizzi et al. (2012), but instead of considering the crops as elliptical hedgerows, we assumed a rectangular canopy shape, which simplifies the trigonometric calculations.

We defined the clumping index as the factor that modifies the leaf area index of a real canopy (F) in a fictitious homogeneous canopy with $\text{LAI}_{\text{eff}} = \Omega(\theta, \phi) \cdot F$ such as its

gap fraction is the same as the gap fraction of the real-world canopy ($G(\theta, \phi)$):

$$\Omega(\theta, \phi) = \frac{-\log[G(\theta, \phi)]}{K_{BE}(\theta)F}, \tag{13}$$

where $K_{BE}(\theta)$ is the beam extinction coefficient through a plant with an ellipsoidal inclination distribution, Eq. (5) (Campbell 1986, 1990), θ is the zenith incident beam angle, and ϕ is the relative azimuth angle between the incidence beam and the row direction.

Our modeled real canopy consists on a horizontally infinite long prism with a total height h_c (i.e., the canopy height) and a width w_c (i.e., canopy width) that is placed above the ground at h_b (i.e., the height of the first living branch). This canopy contains finite-sized leaves randomly placed (no clumping within the canopy) oriented according to an ellipsoidal leaf angle distribution function (Campbell 1990) with a total leaf area index F (Fig. 1).

Then, the real canopy gap fraction is on the sunlit part of the bare soil that is not shaded by the canopy plus the gaps caused by the solar beam passing through the crop canopy:

$$G(\theta, \phi) = f_{sc}(\theta, \phi) \exp[-K_{BE}(\theta)F] + [1 - f_{sc}(\theta, \phi)]. \tag{14}$$

The solar canopy view factor $f_{sc}(\theta, \phi)$ is the fraction of soil that is cast by shadows (Colaizzi et al. 2012) and in our case is estimated as

$$f_{sc}(\theta, \phi) = \frac{w_c + (h_c - h_b)\tan\theta |\sin\phi|}{L}, \tag{15}$$

where L is the row separation (m). For a vertical projection ($\theta = 0$), Eq. (15) reduces to w_c/L, the fractional cover. As opposed to Colaizzi et al. (2012), this clumping index neglects mutual shadowing between adjacent rows.

Clumping index for elliptical hedgerow (C&N–E)

Colaizzi et al. (2012) developed two view factor terms used to calculate τ_C for the elliptical hedgerow approach. These view factors address direct-beam and diffuse irradiance separately. The solar canopy view factor (f_{SC}) is the fraction of canopy visible from the solar beam view angle, and the upward line-integrated hemispherical canopy view factor (f_{UIC}) is the fraction of canopy visible when an upward-looking hemispherical view is integrated from the crop row center to the inter-row center:

$$\begin{aligned} \tau_C = &\, F_{PAR}[W_{DIR,PAR}(f_{SC}\tau_{C,DIR,PAR} + 1 - f_{SC}) \\ &+ W_{DIFF,PAR}(f_{UIC}\tau_{C,DIFF,PAR} + 1 - f_{UIC})] \\ &+ F_{NIR}[W_{DIR,NIR}(f_{SC}\tau_{C,DIR,NIR} + 1 - f_{SC}) \\ &+ W_{DIFF,NIR}(f_{UIC}\tau_{C,DIFF,NIR} + 1 - f_{UIC})]. \end{aligned} \tag{16}$$

The f_{SC} and f_{UIC} terms were developed by Colaizzi et al. (2012) as part of their geometric approach model to account for the unique spatial distribution of row crops, specifically cotton (*Gossypium hirsutum* L.); corn (*Zea mays* L.), and grain sorghum (*Sorghum bicolor* (L.) Moench). The procedures to calculate these terms can be found in Appendix 2 and Appendix 3 of Colaizzi et al. (2012). As described by Colaizzi et al. (2012), f_{SC} is a function of solar zenith and azimuth (relative to crop row orientation) angles, canopy height, canopy width, and row spacing, but not the canopy density which is accounted for by the τ_C term.

For the elliptical hedgerow model, the direct-beam PAR transmittance ($\tau_{C,DIR,PAR}$) was calculated in the same manner as Eq. (5) with an added clumping factor:

$$\tau_{C,DIR,PAR} = \frac{(\rho_{C,PAR}^{*2} - 1)\exp(-\sqrt{\zeta_{PAR}}K_{BE}\eta\text{LAI})}{[(\rho_{C,PAR}^{*}\rho_{S,PAR} - 1) + \rho_{C,PAR}^{*}(\rho_{C,PAR}^{*} - \rho_{S,PAR})\exp(-2\sqrt{\zeta_{PAR}}K_{BE}\eta\text{LAI})]}, \tag{17}$$

where η is a factor calculated using an elliptical geometric approach (Charles-Edwards and Thornley 1973; Annandale et al. 2004) multiplied by the field LAI used to account for the non-random spatial distribution of row crops:

$$\eta = \frac{L}{w_C}P_L M_R, \tag{18}$$

where L is the crop row spacing (m), w_C is the canopy width (m), P_L is the path length fraction of solar beam propagating through a canopy relative to nadir, and M_R is a multiple-row factor that accounts for solar beam traversing across more than one canopy row. Equations for P_L and M_R are found in Appendix 4 of Colaizzi et al. (2012). The $\frac{L}{w_c}$ term coverts the field LAI to a local LAI (i.e., within the canopy row).

4-Stream scattering by arbitrary inclined leaves (4SAIL) model

The 4SAIL model (Verhoef et al. 2007) simulates the absorption, scattering, and transmission processes of a homogeneous turbid plant canopy in both the optical and thermal infrared regions. Optical properties required in 4SAIL are reflectance and transmittance bi-hemispherical factors for a single leaf, as well as soil reflectance factors. In addition, canopy structural parameters needed are leaf area index and a leaf inclination

distribution function. Finally, 4SAIL simulates the hotspot effect near the solar principal plane based on Kuusk (1985).

From the 4SAIL equations described in Verhoef et al. (2007), the downwelling shortwave radiation at the soil level is computed as the sum of the directly transmitted beam radiation $S_s(-1)$ and the scattered diffuse radiation $S^-(-1)$ at soil level. Following the 4SAIL nomenclature, "(0)" and "(−1)" represent the top of the canopy and soil levels, respectively, subscript "s" represents an incoming beam, while superscripts "−" and "+" are the downwelling and upwelling diffuse components:

$$S(-1) = S_s(-1) + S^-(-1), \tag{19}$$

where $S_s(-1)$ and $S^-(-1)$ are computed as

$$S_s(-1) = \tau_{ss} S_s(0) \tag{20a}$$

$$S^-(-1) = \tau_{sd} S_s(0) + \tau_{dd} S^-(0) + \rho_{dd} S^+(-1). \tag{20b}$$

Equation (20a) shows that the solar beam radiation at the top of the canopy is transmitted to the soil by a factor of τ_{ss} (the directional transmittance in the solar beam direction) and τ_{sd} (directional–hemispherical transmittance). On the other hand, the diffuse radiation reaching the soil is the sum of three terms (Eq. 20b): the solar beam radiation $[S_s(0)]$ that reaches the soil after being scattered by the canopy (i.e., the canopy directional–hemispherical transmittance factor, τ_{sd}), the diffuse shortwave radiation $S^-(0)$ at the top of the canopy that is directly transmitted towards the soil by the canopy bi-hemispherical transmittance factor τ_{dd}, and the shortwave radiation leaving the soil $S^+(-1)$ that is scattered back to the soil by the canopy layer by the bi-hemispherical reflectance factor (ρ_{dd}). This latter term represents the additional radiation that reaches the soil due to multiple scattering between the soil and the canopy leaves, with ρ_{dd} the bi-hemispherical reflectance of the canopy. $S^+(-1)$ is finally calculated as

$$S^+(-1) = \frac{\rho_G[(\tau_{ss} + \tau_{sd})S_s(0) + \tau_{dd}S^-(0)]}{1 - \rho_G \rho_{dd}}, \tag{21}$$

where ρ_G is the soil reflectance (assumed Lambertian), and the denominator $(1 - \rho_G \rho_{dd})$ accounts for the multiple scattering between soil and canopy components. The bi-hemispherical reflectance (ρ_{dd}) as well as the canopy transmittances (τ_{ss}, τ_{sd} and τ_{dd}) are internally calculated in 4SAIL Verhoef et al. (2007) based on the optical properties of leaves (leaf reflectance and transmittance) and the canopy structure (effective leaf area index and leaf inclination distribution function). τ_{ss} and τ_{sd}, being directional components, also depend on the solar illumination geometry. In this study, the effective LAI (i.e., $LAI_{eff} = \Omega F$) input in 4SAIL is estimated using the clumping index described in Eqs. (9)–(11), and hence, this approach is named hereinafter as 4SAIL-R.

Discrete anisotropic radiative transfer (DART) model

The DART model (Gastellu-Etchegorry et al. 1996, 2015, 2017; Guillevic and Gastellu-Etchegorry 1999; Gastellu-Etchegorry 2008) simulates radiative transfer from the visible to the thermal infrared parts of the electromagnetic spectrum within heterogeneous canopies characterized by a three-dimensional (3-D) structure. The radiation propagation is tracked with a ray-tracing approach combined with the discrete ordinate method, i.e., radiation can only propagate along a prescribed number of discrete directions. The model predicts surface directional radiance of natural and urban surfaces (i.e., Earth scenes) and the 3-D distribution of radiative energy within the canopy over narrow or wide spectral domains.
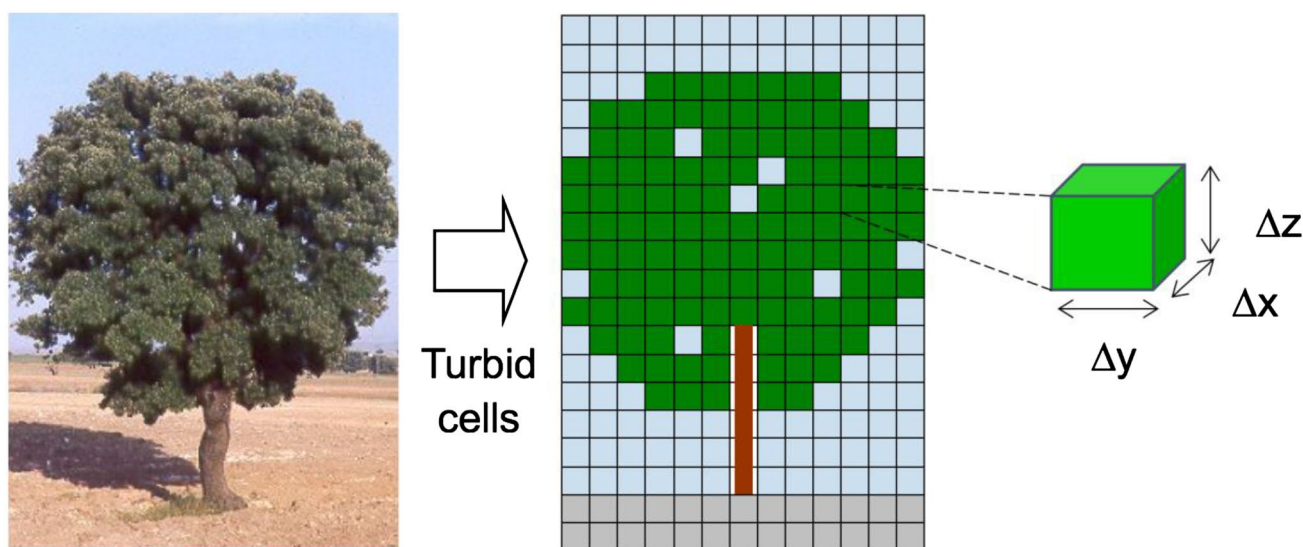

Fig. 2 Vertical section of the 3-D representation of a single tree in the DART model (left)

Fig. 3 Graphic representation of the turbid cell volume scattering: **a** interception points and first-order scattering and **b** second-order scattering
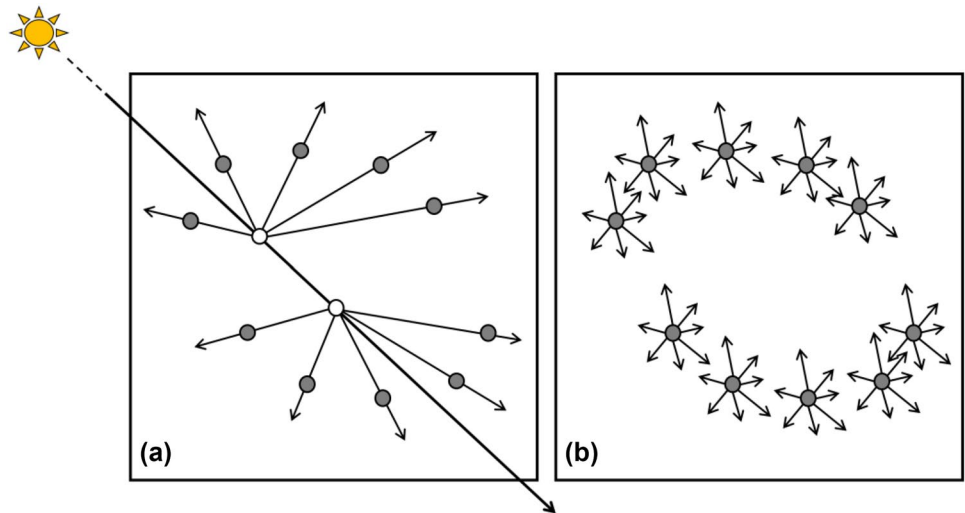

Fig. 4 Predicted vs. observed transmitted solar irradiance for five radiation transfer models. Each point is colored to correspond with the degree of density in the region which it lies. Density is determined on a scale from 0 to 1, with the colors associated with numbers closer to 1 being in the highest density regions, see Table 1 for statistical measurements of model agreement. (Color figure online)
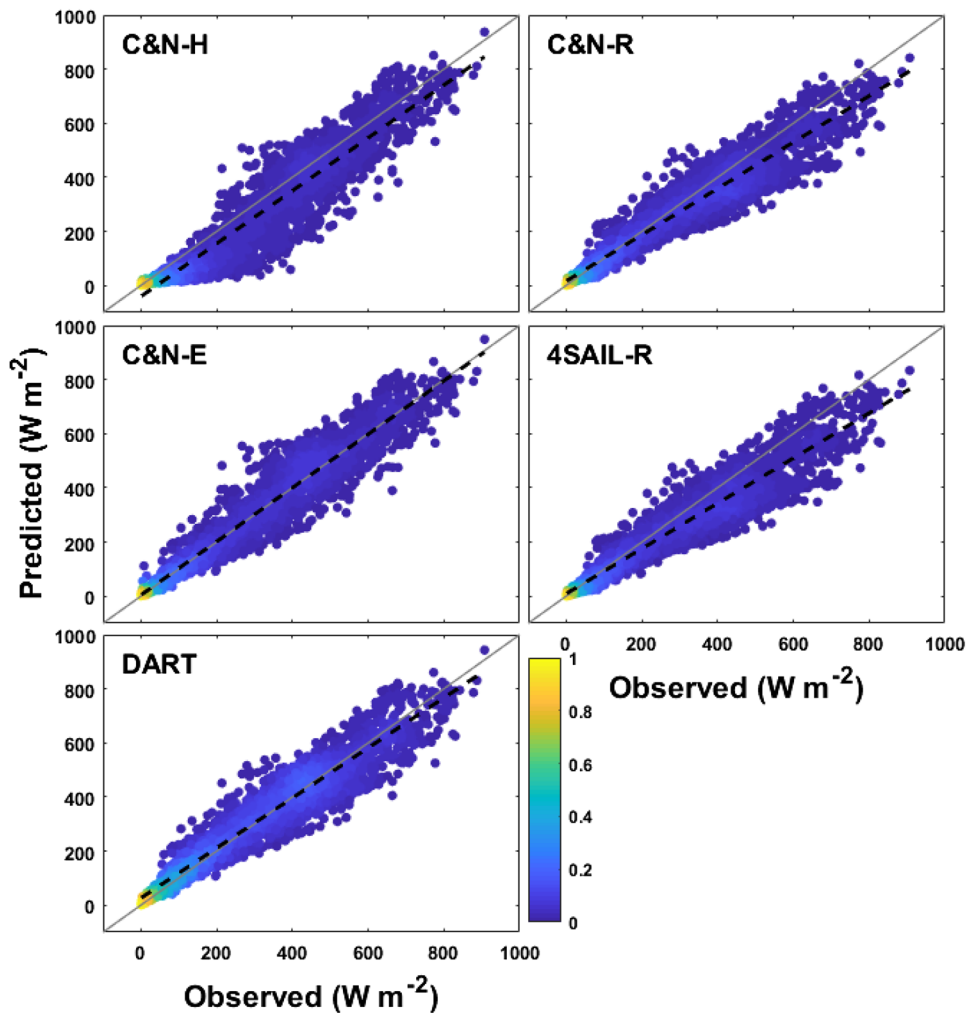
In the DART model, a vegetation scene can be simulated as a 3D distribution of voxels/cells that are filled with turbid medium or as a 3D distribution of facets/triangles is divided into rectangular cells of prescribed dimensions. Each cell represents one of the cover components, such as tree leaves, grass, trunk, and soil (Fig. 2). The main parameters required to describe a natural landscape are the location, shape, and dimension of the trees or plants, and the topography. Depending on

ground data availability, the scene can be represented with varying degrees of complexity. For example, the position and size of the trees can be statistically defined or prescribed for each tree. Leaf cells are characterized by their optical properties (i.e., reflectance and transmittance in the shortwave domain, emissivity in the thermal infrared), leaf area density, and leaf angle distribution. Leaves are represented as small plane elements randomly distributed within leaf cells. For radiative transfer, these leaf cells correspond to turbid media and give rise to volume interaction processes. The soil is represented by opaque media that give rise to surface interaction processes only. In the shortwave domain, DART simulates the radiative transfer within the cover through three major steps: (1) propagation of the direct solar radiation; (2) propagation of the diffuse atmospheric radiation; and (3) multiple scattering of the intercepted radiation by all scene components, i.e., radiation intercepted by scene elements at an iteration is scattered in the next iteration. When a ray crosses a turbid sub-cell, two interception points are computed along its path within the cell (Fig. 3) and will represent the start points for upward scattering and downward scattering, respectively. In this paper, the radiation reaching the soil, i.e., radiation measured by a radiometer installed below the canopy, was estimated by adding the simulated radiation intercepted by the soil layer at each iteration.

The performance of the DART model has been successfully tested using ground-based measurements (Gastellu-Etchegorry et al. 1999) and comparisons to existing 3-D models in the context of the RAdiation transfer Model Intercomparison (RAMI) experiment (Pinty et al. 2004; Widlowski et al. 2013, for example). The model has been successfully used in multiple scientific applications, including surface biophysical parameters' retrieval (Gascon et al. 2004), definition of new satellite sensors requirements, modeling of 3D distribution of photosynthesis and primary production rates in vegetation canopies (Guillevic and Gastellu-Etchegorry 1999), definition of a new chlorophyll index for conifer forests (Malenovský et al. 2013), among others. For additional information about the DART model, please consult Gastellu-Etchegorry et al. (2015) and the web site http://www.cesbio.ups-tlse.fr/dart/#/.

Table 1 Statistical measurements of agreement between observed and predicted transmitted solar irradiance

Parameter	C&N–H	C&N–R	C&N–E	4SAIL–R	DART
ME (W m^{-2})	47	256	−1	39	−2
RMSE (W m^{-2})	87	67	57	77	56
r	0.95	0.96	0.97	0.96	0.97
E_C	0.84	0.90	0.93	0.87	0.94

ME mean error, *RMSE* root mean square error, *r* coefficient of correlation, E_C coefficient of model efficiency

Fig. 5 Predicted vs. observed transmitted solar irradiance for two ▶ Pinot Noir sties in 2015 for four observation periods, see Table 2 for statistical measurements of model agreement

Model evaluation

The agreement between the observed and predicted transmitted solar radiation intensity from the five modeling approaches was assessed using statistical measures [mean error (ME); root mean squared error (RMSE); correlation coefficient (r)] and a modified coefficient of efficiency (E_C) described by Legates and McCabe (1999) and used by Colaizzi et al. (2012) in his model comparison study. The E_C parameter ranges from −1 to 1. An efficiency of one ($E_C = 1$) corresponds to a perfect match of predicted values from the model to the observed data. An efficiency of zero ($E_C = 0$) indicates that the model predictions are as accurate as the mean of the observed data. An efficiency less than zero ($E_C < 0$) indicates that the observed mean is a better predictor than the model (Legates and McCabe 1999; Colaizzi et al. 2012).

For the sensitivity analysis, we varied the canopy inputs (LAI, canopy width, and canopy height) by ± 30% of their base values. Colaizzi et al. (2012) observed a large spatial variability in LAI measurements of up to ± 18%, which was in agreement with the large LAI spatial variability seen by Anderson et al. (2004). Grapevine canopies are less compact in their vegetation distribution than the crops used by Colaizzi et al. (2012) and thus could have a greater variability of canopy input variables. Unless managed, individual grapevines will grow sporadically making it difficult to accurately measure LAI or even canopy width and height, which are key inputs to the radiative transfer models. For this reason, we chose to vary the canopy inputs by 30% which is 5% more than what was used in Colaizzi et al. (2012). Model sensitivity was assessed as

$$\% \text{ change} = \frac{\text{New} - \text{Base}}{\text{Base}}, \tag{22}$$

where % change is the percent change of the newly predicted value ("New" in Eq. 22) from the original ("Base" in Eq. 22) prediction. Base is the original predicted value and New is the predicted value after one of the input variables (LAI, canopy height, and canopy width) has been increased or decreased by 10 or 30%.

Results and discussion

The observed vs. predicted transmitted solar irradiance values had the greatest density (greatest concentration of observed vs. predicted values) at the lowest radiation for all five modeling approaches. As the observed values increased, the predicted values increased in variability and decreased in density
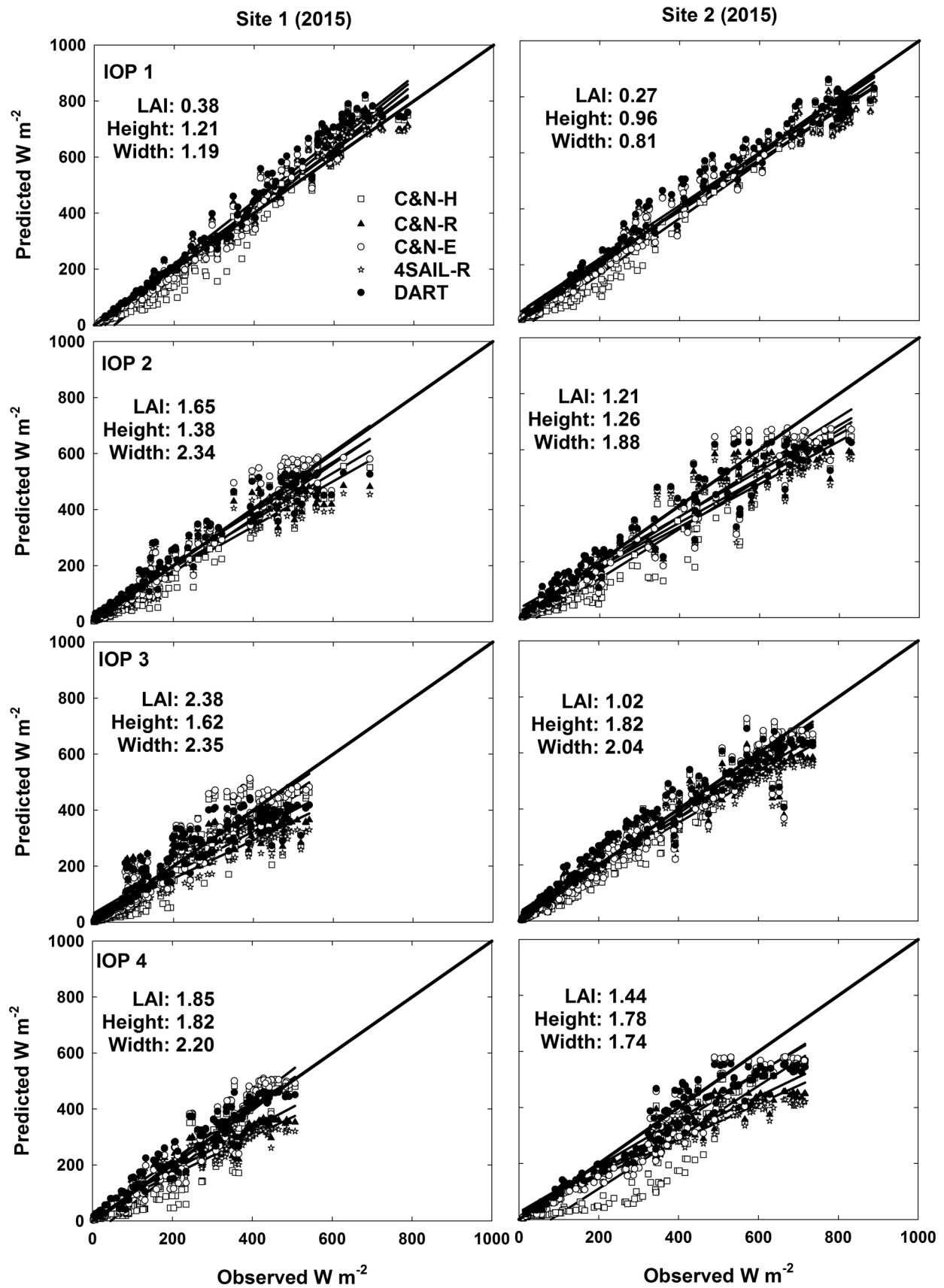
(Fig. 4). The DART model exhibited a denser region from approximately 100–500 W m^{-2} compared to the other four models. Statistical measures of agreement were calculated for the transmitted solar irradiance flux of all years combined and for both vineyard sites using all five radiation transfer models. All E_C values were at least 0.84, which indicated that the models provided a better estimate of the irradiance flux than the means of all measurements. These E_C values agree with the calculated E_C values of Colaizzi et al. (2012) for transmitted solar irradiance through corn, grain sorghum, and cotton for a clumping index approach ($E_C = 0.82$) and an elliptical hedgerow approach ($E_C = 0.84$). All five models had similar coefficient of correlation values, but the C&N–E and DART models had the lowest mean error (around −1 and −2 W m^{-2}) and root mean-squared error (58 and 56 W m^{-2}) values (Table 1).

As expected, the range of observed and predicted transmitted solar radiation decreased in response to increasing canopy size and LAI over the season (Fig. 5). The smaller ranges are associated with more of the downwelling solar radiation being transmitted through the canopy as opposed to radiation reaching the ground unobstructed through canopy row openings. The Campbell and Norman (1998) clumping index model (C&N–H) underestimated transmitted solar radiation to the surface compared to observed values progressively as the canopy dimensions increased over the season (Fig. 5). This suggests that the Campbell and Norman (1998) clumping model does not adequately address the attenuated radiation through the canopy, likely due to the model not adequately predicting the effective LAI. For IOP 4, C&N–H greatly underestimated the observed values when compared with the other four models. This is most likely due to an increased sensitivity of the C&N–H model to the canopy structure input variables (LAI, canopy height, and canopy width) at the latter part of the season as the canopy becomes denser.

Statistical measures of agreement were calculated for the transmitted solar irradiance flux for the 2015 year and all four

Table 2 Statistical measurements of agreement between observed and predicted transmitted solar irradiance for two Pinot Noir sites in 2015 for four intensive observation periods (i.e., IOPs)

Parameter	Site 1					Site 2				
	C&N–H	C&N–R	C&N–E	4SAIL-R	DART	C&N–H	C&N–R	C&N–E	4SAIL–R	DART
IOP1										
ME (W m^{-2})	7	−16	−15	−12	−37	34	4	5	7	−12
RMSE (W m^{-2})	60	40	54	38	59	53	48	39	48	45
r	0.98	0.99	0.99	0.99	0.99	0.99	0.99	0.99	0.99	0.99
E_C	0.93	0.97	0.95	0.97	0.93	0.97	0.97	0.98	0.97	0.97
IOP2										
ME (W m^{-2})	26	13	−4	29	−6	74	45	32	58	27
RMSE (W m^{-2})	57	55	47	64	49	106	89	74	100	80
r	0.97	0.97	0.97	0.97	0.97	0.96	0.96	0.97	0.96	0.96
E_C	0.92	0.92	0.94	0.90	0.94	0.83	0.88	0.92	0.85	0.90
IOP3										
ME (W m^{-2})	23	21	0	40	1	28	17	14	31	−4
RMSE (W m^{-2})	60	67	54	80	56	51	57	47	66	48
r	0.94	0.92	0.94	0.92	0.94	0.98	0.98	0.98	0.98	0.98
E_C	0.86	0.82	0.88	0.75	0.87	0.95	0.94	0.96	0.92	0.96
IOP4										
ME (W m^{-2})	23	30	−14	48	−16	101	78	49	95	34
RMSE (W m^{-2})	65	57	49	74	41	129	109	76	126	68
r	0.95	0.96	0.97	0.96	0.97	0.93	0.96	0.96	0.96	0.96
E_C	0.82	0.86	0.90	0.76	0.92	0.62	0.73	0.87	0.64	0.89

ME mean error, *RMSE* root mean square error, *r* coefficient of correlation, E_C coefficient of model efficiency
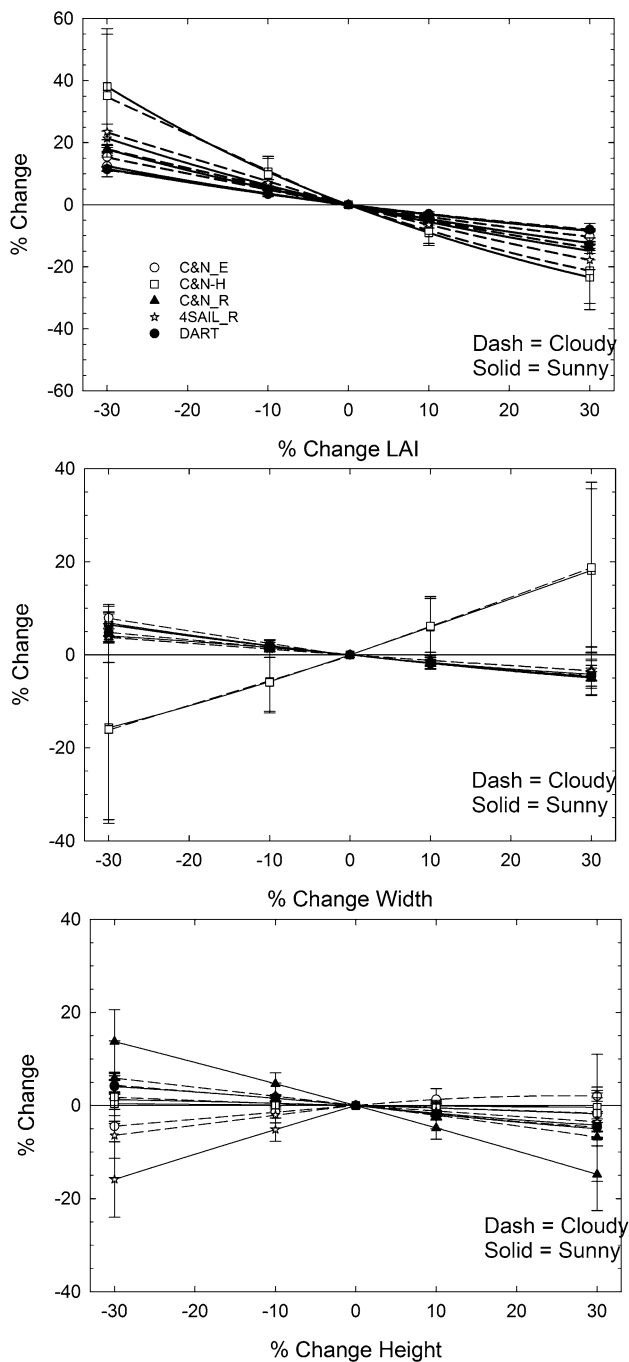
Fig. 6 Sensitivity of models to input parameters (LAI, width, and height) as indicated by % change in predicted values as input parameters are changed by −30, −10, 10, and 30%. Sensitivity analysis was performed for a day with clear skies and a "cloudy" day which had high cloud coverage for the majority of the day. The % change is an average of the percent change of transmitted solar irradiance over the course of a day at 15 min intervals. Error bars are ± one standard deviation of these values

IOPs for both vineyard sites using all five radiation transfer models (Table 2). The E_C values for all five models tended to decrease over the season from IOP1 to IOP 4. This indicates

that the models did a better job at estimating the irradiance flux at the beginning of the season (i.e., low LAI values) compared to the latter part of the season. As suggested by Colaizzi et al. (2012), model sensitivity to the input variables increases as the uncertainty of these variables increases with canopy growth, thus being the most likely reason why the model agreement decreased towards the end of the season.

A sensitivity analysis was performed by altering the LAI, canopy height or canopy width input variables by ± 10% and ± 30% to observe the impact (percent change) in transmitted solar irradiance. Results are shown for a daily averaged % change of average 15 min predicted values for clear and cloudy sky conditions (Fig. 6) and as a diurnal % change (Fig. 7). For both the "cloudy" and "sunny" days, the C&N Heterogeneous model was the most sensitive to changes in LAI and canopy height, whereas the C&N Rectangular Hedgerow model showed the most sensitivity to changes in canopy width (Fig. 6). As suggested by Colaizzi et al. (2012), the sensitivity analysis emphasizes the importance of making accurate LAI, canopy width, and canopy height measurements.

Table 3 lists the statistical measures of agreement between observed and predicted transmitted solar irradiance for 15 min averaged values that were classified as being under "sunny" or "cloudy" conditions in the same manner as the values in Figs. 6 and 7. For both "cloudy" and "sunny" days, the C&N Heterogeneous model shows to be more sensitive to LAI and canopy width than the other models that account for clumping. It is especially sensitive to changes in LAI and canopy width in the morning and evening. C&N heterogeneous shows little sensitivity to changes in canopy width for both "cloudy" and "sunny" days (Fig. 7). The E_C coefficients for the C&N–H, 4SAIL, C&N–E, and DART models for "cloudy" conditions were higher than those calculated for these models under "sunny" conditions. This suggests that these models did a better job at estimating the irradiance flux for "cloudy" or diffuse conditions than for "sunny" or direct radiation conditions. Levashova and Mukhartova (2018) compared the radiative transfer fluxes of a 3D model within a canopy of sparsely planted fruit trees with those simulated by a 1D approach, and showed that for sunny conditions, an application of a simplified 1D approach can result in a significant underestimation of solar radiation, which is consistent with the performance of the DART model shown here (Fig. 7). The C&N–R model had similar E_C coefficients for "cloudy" and "sunny" conditions (0.89 and 0.88, respectively), suggesting that this model performs equally well under either condition.

Conclusions

Five models were used to represent alternative methods to account for the spatial crop row distribution of grapevine canopies. These modeling approaches vary in complexity
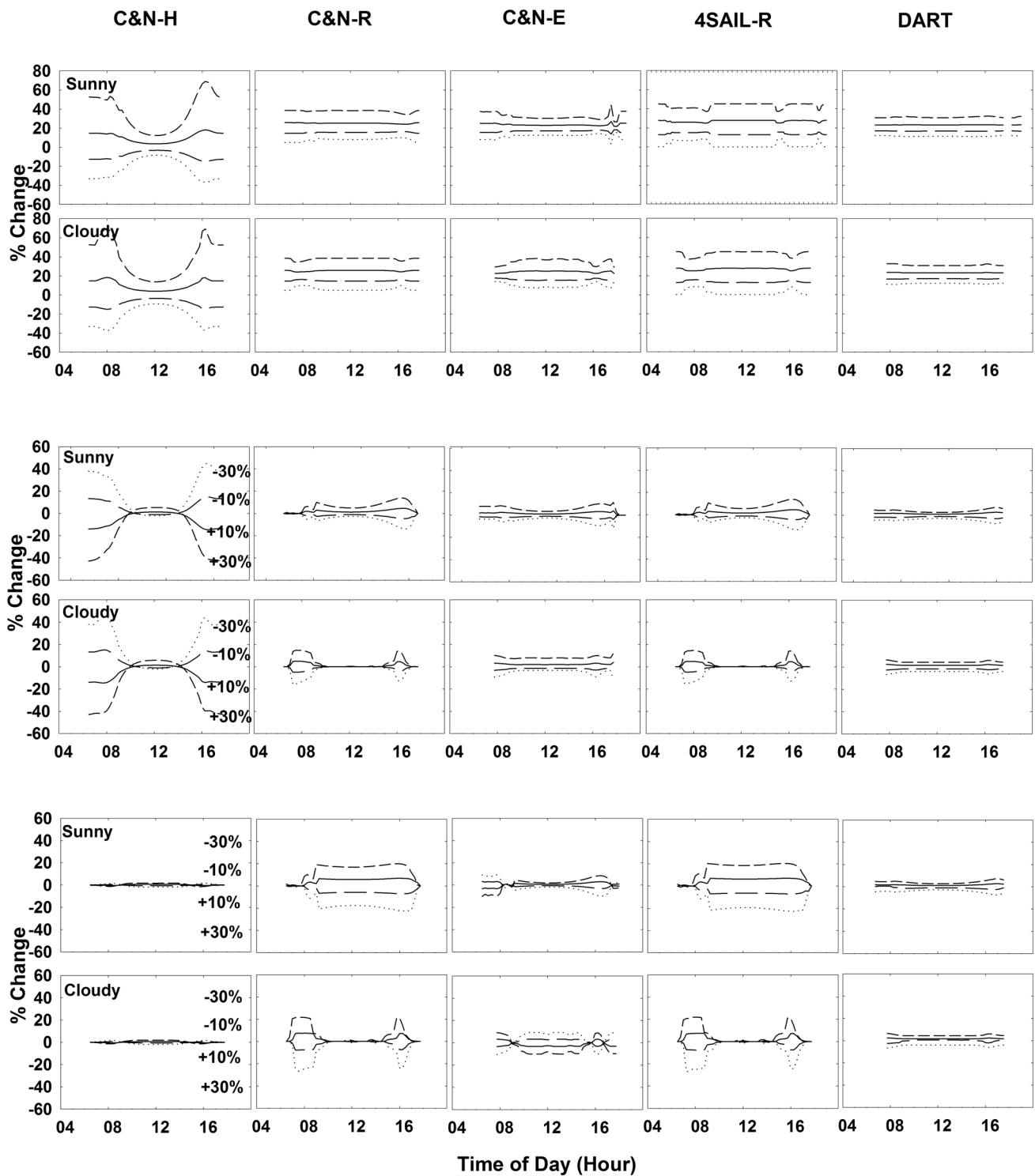
Fig. 7 Diurnal % change in model predicted values as input parameters LAI (top), width (middle), and height (bottom) are changed by −30, −10, 10, and 30%. Sensitivity analysis was performed for a day with clear skies and a "cloudy" day which had high cloud coverage for the majority of the day

of implementation and each has pros and cons associated with ease of use and accuracy. Similarly, the radiation transfer model intercomparison (RAMI) initiative, which proposes a mechanism to benchmark models designed to simulate radiation transfer in plant canopies and over soil surfaces, and other previous comparative studies have shown

Table 3 Statistical measurements of agreement between observed and predicted transmitted solar irradiance for two Pinot Noir sties in 2015 for "sunny" and "cloudy" conditions

Conditions	Parameter	C&N–H	C&N–R	C&N–E	4SAIL–R	DART
Sunny ($n=2448$)	ME (W m^{-2})	53	30	-1	45	-3
	RMSE (W m^{-2})	93	72	62	83	63
	r	0.94	0.95	0.96	0.94	0.95
	E_C	0.80	0.88	0.91	0.84	0.90
Cloudy ($n=383$)	ME (W m^{-2})	11	5	-3	0	-12
	RMSE (W m^{-2})	18	1	13	11	19
	r	0.93	0.96	0.93	0.95	0.94
	E_C	0.73	0.89	0.87	0.90	0.72

Cloudy conditions were determined by the ratio of the predicted transmitted diffuse radiation to observed solar radiation at the ground surface

ME mean error, *RMSE* root mean square error, *r* coefficient of correlation, E_C coefficient of model efficiency

good agreement in some cases and poorer in others (Jacquemoud et al. 2000; Dai and Sun 2007), and also considered differences in model running times and computational needs (Jacquemoud et al. 2000). Our results illustrate the importance of taking into account the non-random spatial distribution of grapevines throughout out the entire season as opposed to other row crops that typically reach a period when the canopy width exceeds the crop row spacing and the clumping factor reaches a value of one before the end of the season [i.e., corn, cotton, and sorghum (Colaizzi et al. 2012)]. Implementation of any of these radiation models into a remote-sensing-based land surface scheme such as the two-source energy balance (TSEB) model when applied at different spatial scales from field up to watershed and regional scales will have different levels of plant canopy information, which is likely to dictate the level of complexity in the canopy radiation partitioning model that can be employed (Anderson et al. 2005). However, based on this analysis, it appears that the C&N Elliptical Hedgerow (C&N–E) and the DART models have the least sensitivity to model input uncertainty and good performance. Jacquemoud et al. (2000) suggested that a good model was a compromise between a few parameters and a good fit for traditional inversion purposes, and also a compromise between a fast running time and good accuracy. Hence, the C&N–E and DART models may be the best candidate to apply in multi-scale modeling approaches such as the remote-sensing-based energy balance model Atmosphere Land EXchange Inverse (ALEXI) and Disaggregation (DisALEXI) schemes for row crops, particularly orchards and vineyards (Semmens et al. 2016). 3D radiative transfer models such as DART are more adaptable to different environmental configurations (e.g., presence of topography), and are usually very accurate provided that the landscape can be accurately characterized, which is not always easy to achieve. Here, we chose to work with a mean 3D vineyard mock-up, but there are other possibilities, such as considering several vineyard mock-ups that are characterized by different configurations (e.g., distance between rows, etc.), and then considering the mean radiation values associated to these different vineyard mock-ups.

References

Allen RG (2005) Environmental and water resources Institute (U.S In: The ASCE standardized reference evapotranspiration equation, American Society of Civil Engineers, Reston, Va

Anderson MC, Neale CMU, Li F, Norman JM, Kustas WP, Jayanthi H, Chavez J (2004) Upscaling ground observations of vegetation water content, canopy height, and leaf area index during SMEX02 using aircraft and Landsat imagery. Remote Sens Environ 92:447–464

Anderson MC, Norman JM, Kustas WP, Li FQ, Prueger JH, Mecikalski JR (2005) Effects of vegetation clumping on two-source model estimates of surface energy fluxes from an agricultural landscape during SMACEX. J Hydrometeorol 6:892–909

Annandale JG, Jovanovic NZ, Campbell GS, Du Sautoy N, Lobit P (2004) Two-dimensional solar radiation interception model for hedgerow fruit trees. Agric For Meteorol 121:207–225

Blonquist JM, Norman JM, Bugbee B (2009) Automated measurement of canopy stomatal conductance based on infrared temperature. Agric For Meteorol 149:2183–2197

Campbell GS (1986) Extinction coefficients for radiation in plant canopies calculated using an ellipsoidal inclination angle distribution. Agric For Meteorol 36(4):317–321

Campbell G (1990) Derivation of an angle density function for canopies with ellipsoidal leaf angle distributions. Agric For Meteorol 49(3):173–176

Campbell GS, Norman JM (1998) An introduction to environmental biophysics, 2nd edn. Springer, New York

Charles-Edwards DA, Thornley JHM (1973) Light interception by an isolated plat: a simple model. Ann Bot 37:919–928

Chen JM, Liu J, Leblan SG, Lacaze R, Roujean JL (2003) Multi-angular optical remote sensing for assessing vegetation structure and carbon absorption. Remote Sens Environ 84:516–525

Colaizzi P, Evett S, Howell T, Li F, Kustas W, Anderson M (2012) Radiation model for row crops: I. Geometric view factors and parameter optimization. Agron J 104(2):225–240

Dai Q, Sun S (2007) A comparison of two canopy radiative models in land surface processes. Adv Atmos Sci 24(3):421–434

French AN, Hunsaker DJ, Clarke TR, Fitzgerald GJ, Luckett WE, Pinter PJ Jr (2007) Energy balance estimation of evapotranspiration for wheat grown under variable management practices in Central Arizona. Trans ASABE 50(6):2059–2071

Gascon F, Gastellu-Etchegorry JP, Lefevre-Fonollosa MJ, Dufrene E (2004) Retrieval of forest biophysical variables by inverting a 3-D radiative transfer model and using high and very high resolution imagery. Int J Remote Sens 25:5601–5616

Gastellu-Etchegorry JP (2008) 3D modeling of satellite spectral images—radiation budget and energy budget of urban landscapes. Meteorol Atmos Phys 102(3–4):187–207

Gastellu-Etchegorry JP, Demarez V, Pinel V, Zagolski F (1996) Modeling radiative transfer in heterogeneous 3D vegetation canopies. Remote Sens Environ 58(2):131–156

Gastellu-Etchegorry JP, Guillevic P, Demarez V, Zagolski F, Trichon V, Deering D, Leroy M (1999) Modeling BRF and radiative regime of tropical and boreal forests—Part I: BRF. Remote Sens Environ 68:281–316

Gastellu-Etchegorry JP, Yin T, Lauret N, Cajgfinger T, Gregoire T, Grau E, Feret JB, Lopes M, Guilleux J, Dedieu G, Malenovský Z, Cook BD, Morton D, Rubio J, Durrieu S, Cazanave G, Martin E, Ristorcelli T (2015) Discrete anisotropic radiative transfer (DART 5) for modeling airborne and satellite spectroradiometer and LIDAR acquisitions of natural and urban landscapes. Remote Sens 7:1667–1701

Gastellu-Etchegorry JP et al (2017) DART: recent advances in remote sensing data modeling with atmosphere, polarization, and chlorophyll fluorescence. IEEE J Sel Top Appl Earth Obs Remote Sens 10:2640–2649. https://doi.org/10.1109/JSTARS.2017.2685528

Goudriaan J (1988) The bare bones of leaf-angle distribution in radiation models for canopy photosynthesis and energy exchange. Agric For Meteorol 43:155–169

Guillevic P, Gastellu-Etchegorry JP (1999) Modeling BRF and radiative regime of tropical and boreal forests—part II: PAR regime. Remote Sens Environ 68:317–340

Howell TA, Steiner JL, Evett SR, Schneider AD, Copeland KS, Dusek DA, Tunick A (1993) Radiation balance and soil water evaporation of bare Pullman clay loam soil. In: Allen RG, Neale CMU (eds) Management of irrigation and drainage systems: integrated perspectives. American Society of Civil Engineering, New York, pp 922–929 In

Jacquemoud S, Bacour C, Poilvé H, Frangi JP (2000) Comparison of four radiative transfer models to simulate plant canopies reflectance: direct and inverse mode. Remote Sens Environ 74:471–481

Kustas WP, Norman JM (1999) Evaluation of soil and vegetation heat flux predictions using a simple two-source model with radiometric temperatures for partial canopy cover. Agric For Meteorol 94(1):13–29

Kustas WP, Agam N, Alfieri JG, McKee LG, Prueger JH, Hipps L, Howard AM, Heitman J (2018) Below canopy radiation divergence in a vineyard: implications on interrow surface energy balance. Irrig Sci. https://doi.org/10.1007/s00271-018-0601-0

Kuusk A (1985) The hot spot effect of a uniform vegetative cover. Sov J Remote Sens 3(4):645–658

Legates DR, McCabe GJ Jr (1999) Evaluating the use of "goodness-of fit" measures in hydrologic and hydroclimatic model validation. Water Resour Res 35:233–241

Levashova NT, Mukhartova YV (2018) A three-dimensional model of solar radiation transfer in a non-uniform plant canopy. IOP Conf Ser Earth Environ Sci 107:012101

Li F, Kustas WP, Prueger JH, Neale CMU, Jackson TJ (2005) Utility of remote sensing-based two-source energy balance model under low and high-vegetation cover conditions. J Hydrometeorol 6:878–891

Malenovský Z, Homolová L, Zurita-Milla R, Lukeš P, Kaplan V, Hanuš J, Gastellu-Etchegorry JP, Schaepman ME (2013) Retrieval of spruce leaf chlorophyll content from airborne image data using continuum removal and radiative transfer. Remote Sens Environ 131:85–102

McCree KJ (1972) Test of current definitions of photosynthetically active radiation against leaf photosynthesis data. Agric Meteorol 10:443–453

Meek DW, Hatfield JL, Howell TA, Idso SB, Reginato RJ (1984) A generalized relationship between photosynthetically active radiation and solar radiation. Agron J 76:939–945

Nouvellon Y, Bégué A, Moran MS, Lo Seen D, Rambal S, Luquet D, Chehbouni G, Inoue Y (2000) PAR extinction in shortgrass ecosystems: effects of clumping, sky conditions and soil albedo. Agric For Meteorol 105(1–3):21–41

Pieri P (2010a) Modelling radiative balance in a row-crop canopy: row–soil surface net radiation partition. Ecol Model 221:791–801

Pieri P (2010b) Modelling radiative balance in a row-crop canopy: cross-row distribution of net radiation at the soil surface and energy available to clusters in a vineyard. Ecol Model 221:802–811

Pinty B, Widlowski JL, Taberner M, Gobron N, Verstraete M, Disney M, Gascon F, Gastellu JP, Jiang L, Kuusk A (2004) Radiation transfer model intercomparison (RAMI) exercise: results from the second phase. J Geophys Res Atmos. https://doi.org/10.1029/2003JD004252

Semmens KA, Anderson MC, Kustas WP, Gao F, Alfieri JG, McKee L, Prueger JH, Hain CR, Cammalleri C, Yang Y, Xia T, Sanchez L, Alsina MM, Vélez M (2016) Monitoring daily evapotranspiration over two California vineyards using Landsat 8 in a multi-sensor data fusion approach. Remote Sens Environ 185:155–170

Tunick A, Rachele H, Hansen FV, Howell TA, Steiner JL, Schneider AD, Evett SR (1994) REBAL'92: a cooperative radiation and energy balance field study for imagery and electromagnetic propagation. Bull Am Meteorol Soc 75:421–430

Verhoef W, Jia L, Xiao Q, Su Z (2007) Unified optical-thermal four-stream radiative transfer theory for homogeneous vegetation canopies. IEEE Trans Geosci Remote Sens 45(6):1808–1822

Weiss A, Norman JM (1985) Partitioning solar radiation into direct and diffuse, visible, and near-infrared components. Agric For Meteorol 34:205–213

Widlowski JL, Pinty B, Lopatka M, Atzberger C, Buzica D, Chelle M, Disney M, Gastellu-Etchegorry JP, Gerboles M, Gobron N (2013) The fourth radiation transfer model intercomparison (RAMI-IV): proficiency testing of canopy reflectance models with ISO-13528. J Geophys Res Atmos 118:6869–6890